Proc. of the X Int. Conf. — Ion Implantation and other Applications of Ions and Electrons, Kazimierz Dolny 2014

Influence of Defects Introduced by Irradiation with 4–9 MeV Helium Ions on Impedance of Silicon Diodes

N.A. Poklonski[a], N.I. Gorbachuk[a], Vo Quang Nha[a], S.V. Shpakovski[b], V.A. Filipenya[b], V.A. Skuratov[c], T.N. Kołtunowicz[d,*], N. Kukharchyk[e], H.-W. Becker[e] and A. Wieck[e]

[a]Belarusian State University, 4 Nezavisimosti Pr., BY-220030, Minsk, Belarus
[b]JSC "INTEGRAL", 121A Kazintsa Str., BY-220108, Minsk, Belarus
[c]Joint Institute for Nuclear Research, 6 Joliot-Curie Str., RU-141980 Dubna, Russia
[d]Lublin University of Technology, Nadbystrzycka 38d, 20-618 Lublin, Poland
[e]Ruhr-University Bochum, 150 Universitaets Str., D-44780 Bochum, Germany

Silicon diodes irradiated with helium ions with energies of 4.1, 6.8 and 8.9 MeV are studied. It is shown that the mechanism determining the behaviour of frequency dependence of complex electric module and correspondingly the behavior of impedance of diodes irradiated with helium ions in the frequency region 3–200 kHz is a recharging of vacancy complexes localized in the space charge region.

DOI: 10.12693/APhysPolA.128.891
PACS: 72.20.Jv, 61.80.Fe

1. Introduction

Irradiation with helium ions has been successfully applied for increasing the operation speed of bipolar semiconductor devices [1] for a long time. By changing the energy of helium ion irradiation one can change the depth of irradiation damaged layer. This allows to control such parameters as reverse recovery time and reverse currents [1–3]. There are also possible changes in the frequency dependences of impedance. Study of features of impedance frequency dependences caused by variation of irradiation energy are of interest for evolution of radiation technologies of semiconductor materials modification as well as for improving capacitance research methods of semiconductor barrier structures formed on high-resistance substrates.

The purpose of this work is to study the effect of irradiation-induced defects introduced by helium ion irradiation on dependences of impedance Z of diodes on frequency f of alternate current.

2. Experimental technique

The diodes were manufactured on the uniformly phosphorous doped single-crystalline silicon wafers with resistivity of 90 Ω cm and the 460 μm thickness. The p^+-type anode region was formed by boron ion implantation. The active area of the p^+–n-junction was 4.41 mm^2. The p^+–n-junction was located at $x_j \approx 3$ μm. This agrees with the results of boron diffusion simulation. The calculated distribution profile of the difference $|N_A - N_D|$ is shown in the inset of Fig. 1 (curve 1). Being estimated from the measurements of the capacitance–voltage characteristics, a double electrical layer thickness of the p^+–n-junction (space charge region) in the as-manufactured diodes was found to be ≈4.5 μm at room temperature and $U = 0$. The contacts were formed by Al sputtering (contact thickness to p^+-region was 1.5 μm).

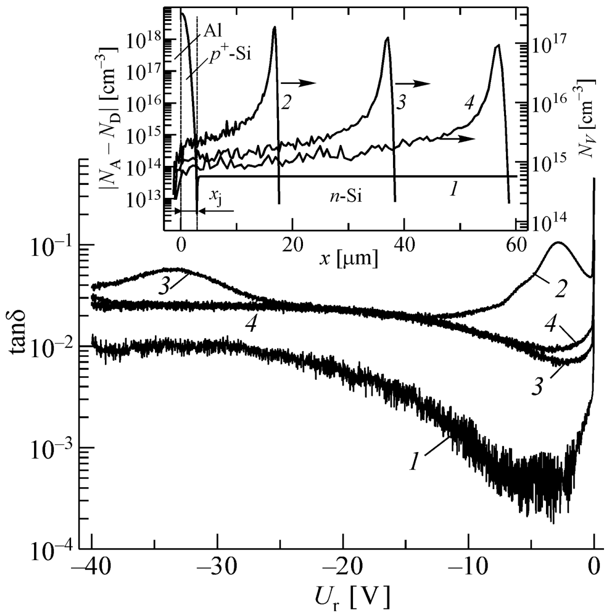

Fig. 1. Dielectric loss tangent $\tan\delta$ as a function of reverse bias voltage U_r for the virgin diodes (1), and for those irradiated with helium ions with the energies 4.1 MeV (2), 6.8 MeV (3) and 8.9 MeV (4). The irradiation fluence is 10^{11} cm^{-2}. Inset: distribution profile of the difference $|N_A - N_D|$ of the concentrations of acceptors and donors (curve 1) and distribution profiles of primary vacancies introduced by helium ion irradiation with the fluence of 10^{11} cm^{-2} and the energy of 4.1 MeV (curve 2), 6.8 MeV (3) and 8.9 MeV (4).

The diodes were irradiated with helium ions from the p^+-region side. Ion energy was 4.1, 6.8, and 8.9 MeV.

*corresponding author; e-mail: t.koltunowicz@pollub.pl

The calculated distribution profiles of primary vacancies formed due to helium ion irradiation are shown in the inset of Fig. 1. The distance δ between the boundary of space charge region and the maximum of concentration of primary vacancies was 9, 19, and 49 μm, respectively.

Measurements of frequency dependences of the real Z' and imaginary Z'' parts of the impedance $Z' + \mathrm{i}Z''$ were performed with the use of an Agilent E4980A LCR-meter at room temperature in the frequency range from 2 Hz to 2 MHz. The investigations were carried out for the diodes irradiated with helium ions with a fluence of 10^{11} cm^{-2}.

Deep level transient spectroscopy (DLTS) measurements were made at the frequency of 1 MHz with the use of a spectrometer CE-6 (OMNITEL, Minsk). The trap filling voltage was 0 V, the trap emission voltage was -10 V. The measurements were performed for diodes irradiated with helium ions with a fluence of 10^{10} cm^{-2}.

3. Experimental results and discussion

The DLTS spectra are shown in Fig. 2 for the virgin diodes (1) and for those irradiated with helium ions (2–4). In the DLTS spectra of virgin diodes two peaks E4 and E5 are observed. These peaks correspond to the trap levels $E_c-(0.45 \pm 0.03)$ eV and $E_c-(0.51 \pm 0.03)$ eV. Occurrence of the peaks in the DLTS spectra of the virgin diodes can be attributed to technologically introduced defects during manufacturing of diodes. For the diodes irradiated with helium ions, the trap energy levels in the band gap corresponding to the peaks E1, E2, and E3 were not virtually dependent on irradiation energy and were $E_c-(0.19 \pm 0.02)$ eV (for E1 peak); $E_c-(0.25 \pm 0.02)$ eV (for E2) and $E_c-(0.40 \pm 0.03)$ eV (for E3). Comparison of these results with the known data [2–6] allows to assume that for the E1 peak A-centers are responsible (i.e. the complexes "oxygen atom–vacancy" — $\mathrm{VO}^{(-/0)}$) and the complexes "interstitial carbon atom–site carbon atom" ($\mathrm{C_iC_s^{(-/0)}}$), and for the E2 peak — divacancies ($\mathrm{V_2^{(=/-)}}$).

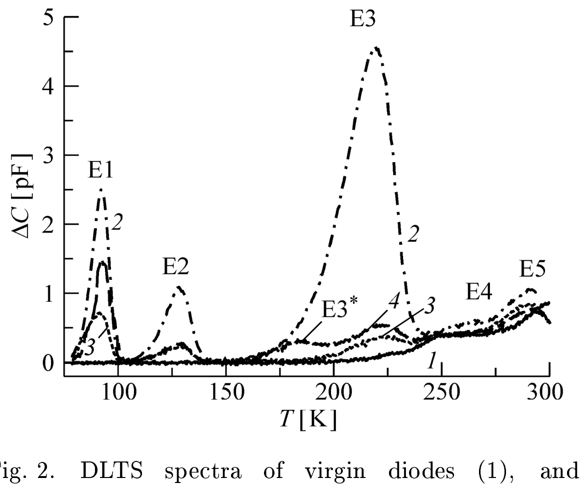

Fig. 2. DLTS spectra of virgin diodes (1), and diodes irradiated with helium ions with the energies 4.1 MeV (curve 2), 6.8 MeV (3) and 8.9 MeV (4). The irradiation fluence is 10^{10} cm^{-2}.

The E3 peak for the diodes irradiated with helium with the energies 4.1 and 6.8 MeV is superposition of signals from the divacancies ($\mathrm{V_2^{(-/0)}}$) and the multi-vacancy complexes: e.g., a complex of divacancy with oxygen $\mathrm{V_2O^{(=/-)}}$ [7] or trivacancy $\mathrm{V_3^{(=/-)}}$ [8]. The E3* peak (along with the E3 peak) is also observed in the DLTS spectra of diodes irradiated with 8.9 MeV helium ions. We cannot find energy level position corresponding to the E3* peak. It should be noted that the E3 peak amplitude in the DLTS spectra of diodes irradiated with 4.1 MeV helium ions exceeds essentially the amplitude of the E3 peak in the spectra of diodes irradiated with 6.8 or 8.9 MeV helium ions.

Figure 1 shows the dielectric loss tangent $\tan\delta$ as a function of the reverse bias voltage U_r measured at the frequency 1 kHz for the virgin diodes (curve 1) and for the helium irradiated diodes (curves 2–4). There are maxima in the dependences 2 and 3. The maximum for the diodes irradiated with 4.1 MeV helium ions (curve 2) is observed at the voltage $U_m = -2.9$ V, and for 6.8 MeV helium ions (curve 3) — at the voltage $U_m = -33.5$ V. Nonmonotonic behaviour of $\tan\delta(U_\mathrm{r})$ is attributed to the expansion of space charge region into the base. In the process of capturing of the irradiation damaged layer by the space charge region, the increases in the generation currents [9] and in the losses induced by defect recharging [10] are observed.

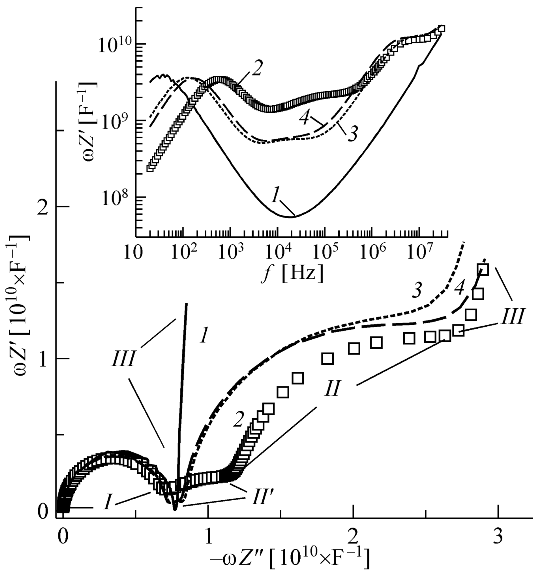

Fig. 3. Complex plane plots of the complex electric module M/C_0 for the virgin diodes (1), and for those irradiated with helium ions with the energies 4.1 MeV (curve 2), 6.8 MeV (3) and 8.9 MeV (4). The irradiation fluence is 10^{11} cm^{-2}. Inset: frequency dependence of the imaginary part of the complex electric module.

Figure 3 shows the plots of M^* in a complex plane for the virgin diodes (curve 1) and for those diodes irradiated with helium ions with the fluence of 10^{11} cm^{-2}

(plots 2–4). The quantity M^* is proportional to the complex electric module M and is defined as $M^* = M/C_0 = \omega(-Z'' + \mathrm{i}\,Z')$, where C_0 is the geometrical capacitance of a vacuum capacitor having the geometry identical to that of the examined sample, $\omega = \pi f$ is the angular frequency. From the point of view of physics, M^* is the quantity inverse to the diode capacity [11]. For short, the quantity M^* is further referred to as the complex electric module. The inset in Fig. 3 shows the dependence of the imaginary part of $M^* = M/C_0$ (i.e. $\omega Z'$) on the frequency f of the alternate current.

In the complex plane plots of complex electric module for the diodes irradiated with helium ions one can distinguish four arcs. The most visible arcs appear in the plots corresponding to the diodes irradiated with 4.1 MeV helium ions. In Fig. 3 they are designated with the Roman numbers I, II, II' and III. In contrast to the irradiated diodes, in the plot of the virgin diodes one can tell only two arcs (I and III). The presence of several arcs in the complex plane plots of complex electric quantities (impedance, admittance etc.) is a sign pointing to the presence of several relaxation time constants [11]. In the case of the absence of irradiation-induced defects, the equivalent circuit of a silicon diode can be represented by two serially connected parallel *RC*-circuits [12]. Thus, it can be assumed that arcs *I* and *III* in the complex plane plot of complex electric module correspond to the space charge region and to the diode base.

Arc *II* in the complex plane plots of all irradiated diodes is observed equally clearly. While arc II' for the diodes irradiated with 6.8 and 8.9 MeV helium ions is weakly expressed and virtually coincides with each other. Also strong difference in the frequency range 3–200 kHz of the dependences $\omega Z'(f)$ for the diodes irradiated with 4.1 MeV helium ions from the ones for the diodes irradiated with 6.8 and 8.9 MeV helium ions is of significant importance.

At the irradiation fluences of 10^{11} cm^{-2} a strong compensation of doping impurity in the base by irradiation-induced defects is possible [9]. Thus, appearance of arcs *II* and *II'* in the complex plane plots of irradiated diodes can be attributed to the recharging of the irradiation-induced defects as well as to the presence of the irradiation damaged layer. Nevertheless, as it follows from the data shown in the inset of Fig. 1, in the vicinity of the average projective range the local concentration of the primary vacancies introduced by helium ion irradiation with the energies ranged 4–9 MeV differs insignificantly. The close values of the resistance (800–600 Ω) in the frequency range 0.4–2 MHz argue that the effectiveness of irradiation-induced defect introduction is almost the same for the energy values used in the experiment. On the other hand, in the space charge region the local concentration of the primary vacancies of the diodes irradiated with 4.1 MeV helium ions exceeds the local concentration for those irradiated with the energies 6.8 and 8.9 MeV nearly by the order of magnitude. Thus, it can be assumed that arc *II* in the complex plane plots of complex electric module is attributed to the effect of the irradiation damaged layer, and arc *II'* is caused by the time-lag of recharging of irradiation-induced defects localized in the space charge region. The DLTS data confirm implicitly this assumption (see Fig. 2). Dielectric losses of diodes increase exactly in the case (see Fig. 1) when the space charge region captures the irradiation damaged region. This agrees also with the results [10, 12] and can be considered as an additional support for the stated assumption.

4. Conclusions

It is shown that the mechanism determining the behaviour of frequency dependence of complex electric module and correspondingly that of impedance of diodes irradiated with helium ions in the frequency region 3–200 kHz is recharging of vacancy complexes localized in the space charge region.

Acknowledgments

This paper was prepared with the financial support of Belarusian Scientific program "Electronics and Photonics" (task 1.1.03) and the German Academic Exchange Service DAAD.

References

[1] V. Kozlovski, V. Abrosimova, *Radiation Defect Engineering*, World Sci., Singapore 2005.

[2] P. Hazdra, V. Komarnitskyy, *Microelectron. J.* **37**, 197 (2006).

[3] P. Hazdra, J. Vobecký, H. Dorschner, K. Brand, *Microelectron. J.* **35**, 249 (2004).

[4] V. Eremin, E. Verbitskaya, Z. Li, *Nucl. Instrum. Methods Phys. Res. A* **476**, 537 (2002).

[5] R. Siemieniec, F.-J. Niedernostheide, H.-J. Schulze, W. Südkamp, U. Kellner-Werdehausen, J. Lutz, *J. Electrochem. Soc.* **153**, G108 (2006).

[6] V.P. Markevich, O. Andersen, I.F. Medvedeva, J.H. Evans-Freeman, I.D. Hawkins, L.I. Murin, L. Dobaczewski, A.R. Peaker, *Physica B* **308–310**, 513 (2001).

[7] M. Mikelsen, E.V. Monakhov, G. Alfieri, B.S. Avset, J. Härkönen, G. Svensson, *J. Phys. Condens. Matter* **17**, S2247 (2005).

[8] V.P. Markevich, A.R. Peaker, S.B. Lastovskii, L.I. Murin, J. Coutinho, V.J.B. Torres, P.R. Briddon, L. Dobaczewski, E.V. Monakhov, B.G. Svensson, *Phys. Rev. B* **80**, 235207 (2009).

[9] A.G. Milnes, *Deep Impurities in Semiconductors*, Wiley, New York 1973.

[10] N.A. Poklonski, N.I. Gorbachuk, S.V. Shpakovski, S.B. Lastovskii, A. Wieck, *Semiconductors* **44**, 380 (2010).

[11] *Impedance Spectroscopy: Theory Experiment and Applications*, Eds. E. Barsoukov, J.R. Macdonald, Wiley, New York 2005.

[12] N.A. Poklonski, N.I. Gorbachuk, S.V. Shpakovski, A. Wieck, *Techn. Phys.* **55**, 1463 (2010).